

Study of charmed baryons at Belle

Anna Vinokurova^{*†}

Budker Institute of Nuclear Physics and Novosibirsk State University, Russia

E-mail: vinokurovanna@gmail.com

We report measurements of the branching fractions of the decays $\Lambda_c^+ \rightarrow \Sigma^+ \pi^- \pi^+$, $\Lambda_c^+ \rightarrow \Sigma^0 \pi^+ \pi^0$ and $\Lambda_c^+ \rightarrow \Sigma^+ \pi^0 \pi^0$ relative to the reference channel $\Lambda_c^+ \rightarrow p K^- \pi^+$ [1]. The charmed-strange baryon $\Xi_c(2930)^0$, decaying to $K^- \Lambda_c^+$, is observed for the first time in $B^- \rightarrow K^- \Lambda_c^+ \bar{\Lambda}_c^-$ decays. We also measure $\mathcal{B}(B^- \rightarrow K^- \Lambda_c^+ \bar{\Lambda}_c^-)$ with improved precision, and search for the charmonium-like state $Y(4660)$ and its spin partner, Y_η , in the $\Lambda_c^+ \bar{\Lambda}_c^-$ invariant mass spectrum [2]. Decays of the Ω_c^0 charmed baryon into hadronic final states were studied[3]. We present the results of a study of excited Ω_c charmed baryons in the decay mode $\Xi_c^+ K^-$ [4].

XIV International Conference on Heavy Quarks and Leptons (HQL2018)

May 27- June 1, 2018

Yamagata Terrsa, Yamagata, Japan

^{*}Speaker.

[†]on behalf of the Belle collaboration

All the following analyses are based on the full data sample collected by the Belle detector [5] at the KEKB asymmetric-energy e^+e^- collider [6]. For sections 1 and 2 the data are collected at and near the $\Upsilon(4S)$ resonance, corresponding to an integrated luminosity of 711 fb^{-1} . For sections 3 and 4 the analyses also include the Belle data taken at beam energies corresponding to the other Υ resonances and the nearby continuum ($e^+e^- \rightarrow q\bar{q}$, where $q \in \{u, d, s, c\}$), corresponding to an integrated luminosity of 980 fb^{-1} .

1. Measurement of the decays $\Lambda_c \rightarrow \Sigma\pi\pi$

The Λ_c , which is the lightest charmed baryon and has a udc quark configuration, plays a key role in the study of charmed baryons. As most Λ_b^0 decays include a Λ_c^+ in their decay products, improved measurements of Λ_c^+ hadronic branching fractions help to constrain fragmentation functions of bottom, as well as charm, quarks through the measurement of inclusive heavy-flavor baryon production. The recent model-independent measurements of the normalization mode $\Lambda_c \rightarrow pK\pi$ by Belle [7] and BESIII [8] improve the accuracy of Λ_c^+ branching fractions measured relative to this mode. The decay $\Lambda_c^+ \rightarrow \Sigma\pi\pi$ is particularly interesting as it has been proposed as a possible avenue to extract the $\Sigma - \pi$ scattering length, and this measurement would provide crucial information in the study of the $\Lambda(1405)$ resonance.

We report measurements of the branching fractions of the decays $\Lambda_c^+ \rightarrow \Sigma^+\pi^-\pi^+$, $\Lambda_c^+ \rightarrow \Sigma^0\pi^+\pi^0$ and $\Lambda_c^+ \rightarrow \Sigma^+\pi^0\pi^0$ relative to the reference channel $\Lambda_c^+ \rightarrow pK^-\pi^+$.

The signal yields are extracted using an unbinned extended maximum-likelihood fit to the Λ_c -candidate invariant-mass distribution. To extract the signal yields in a model-independent way, the Dalitz distribution of each decay is binned and independent fits are performed in each bin. The binning and the Dalitz-bin efficiencies for $\Lambda_c^+ \rightarrow \Sigma^0\pi^+\pi^0$ (as an example) are shown in Fig. 1. Figure 2 shows sample Dalitz-bin plot for the same channel to illustrate the extraction of the signal yields.

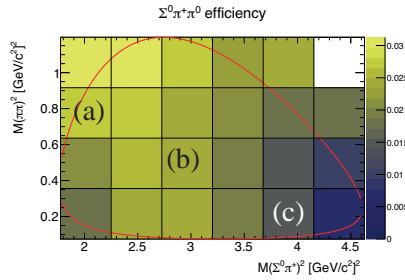


Figure 1: Dalitz distribution binning and reconstruction efficiency in bins of $M(\Sigma^0\pi^+)^2$ vs. $M(\pi^0\pi^+)^2$ for the $\Lambda_c^+ \rightarrow \Sigma^0\pi^+\pi^0$ channel. The red curved line is the kinematic boundary of the Dalitz plot. The fits in representative bins (a), (b) and (c) are shown in Fig. 2.

The branching fractions of the decays $\Lambda_c^+ \rightarrow \Sigma^+\pi^-\pi^+$, $\Lambda_c^+ \rightarrow \Sigma^0\pi^+\pi^0$, and $\Lambda_c^+ \rightarrow \Sigma^+\pi^0\pi^0$ relative to that of the decay $\Lambda_c^+ \rightarrow pK^-\pi^+$ are calculated from the total efficiency-corrected signal yields and given in Table 1.

The results agree with previous experimental findings where they exist. This is the first measurement of $\Lambda_c^+ \rightarrow \Sigma^+\pi^0\pi^0$. The measurement of $\Lambda_c^+ \rightarrow \Sigma^0\pi^+\pi^0$ is four times more precise than the current world average.

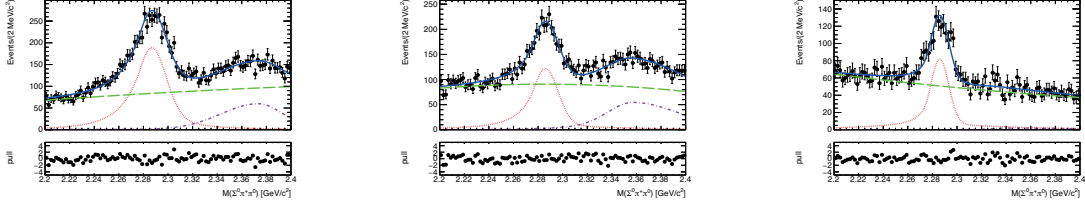


Figure 2: Fits (solid blue curves) in three representative Dalitz bins for the $\Lambda_c^+ \rightarrow \Sigma^0 \pi^+ \pi^0$ channel. From left to right, the panels correspond to bins (a), (b), and (c) in Fig. 1. The signal is shown as the red dotted curve and the combinatorial background as the green dashed curve. The pull distribution of the fit is shown at the bottom of each panel.

Final state	$\mathcal{B}(\Sigma\pi\pi)/\mathcal{B}(pK\pi)$	$\mathcal{B}(\Sigma\pi\pi)$ [%]	$\mathcal{B}_{WA}(\Sigma\pi\pi)$ [%]
$\Sigma^+ \pi^- \pi^+$	$0.706 \pm 0.003 \pm 0.030$	$4.48 \pm 0.02 \pm 0.19 \pm 0.23$	4.57 ± 0.29
$\Sigma^0 \pi^+ \pi^0$	$0.491 \pm 0.005 \pm 0.023$	$3.12 \pm 0.03 \pm 0.15 \pm 0.16$	2.3 ± 0.9
$\Sigma^+ \pi^0 \pi^0$	$0.198 \pm 0.006 \pm 0.017$	$1.26 \pm 0.04 \pm 0.11 \pm 0.07$	-

Table 1: Branching fraction measurements. The third column lists the absolute branching fractions taking $\mathcal{B}(\Lambda_c^+ \rightarrow pK^- \pi^+) = 6.35 \pm 0.33$ % [9]. Errors are statistical, systematic, and from $\mathcal{B}(pK\pi)$, respectively. In the final column, the current world average is given.

2. Observation of $\Xi_c(2930)^0$ and updated measurement of $B^- \rightarrow K^- \Lambda_c^+ \bar{\Lambda}_c^-$

The $\Xi_c(2930)$ charmed-strange baryon has been reported only in the analysis of $B^- \rightarrow K^- \Lambda_c^+ \bar{\Lambda}_c^-$ by BaBar [10], where they claim a signal in the $K^- \Lambda_c^+$ invariant mass distribution. However, neither the results of the fit to their spectrum nor the significance of the signal were given; the Particle Data Group (PDG) lists it as a “one star” state [9]. The same B decay mode can be used to study the $\Lambda_c^+ \bar{\Lambda}_c^-$ invariant mass. In this system, Belle has previously observed a charmonium-like state, the $Y(4630)$, in the initial-state radiation (ISR) process $e^+e^- \rightarrow \gamma_{\text{ISR}} \Lambda_c^+ \bar{\Lambda}_c^-$ [11]. As this mass is very close to that of the $Y(4660)$ observed by Belle in the ISR process $e^+e^- \rightarrow \gamma_{\text{ISR}} \pi^+ \pi^- \psi'$ [12], many theoretical explanations assume they are the same state. If the $Y(4660)$ is modeled as an $f_0(980)\psi'$ bound state, it is predicted that it should have a spin partner – an $f_0(980)\eta_c(2S)$ bound state denoted as the Y_η – with a mass and width of 4613 ± 4 MeV/ c^2 and around 30 MeV, respectively, and a large partial width into $\Lambda_c^+ \bar{\Lambda}_c^-$ [13].

We reconstruct the Λ_c^+ via the $\Lambda_c^+ \rightarrow pK^- \pi^+$, pK_S^0 , $\Lambda\pi^+$, $pK_S^0 \pi^+ \pi^-$, and $\Lambda\pi^+ \pi^+ \pi^-$ decay channels. When a Λ_c^+ and $\bar{\Lambda}_c^-$ are combined to reconstruct a B candidate, at least one is required to have been reconstructed via the $pK^+ \pi^-$ or $\bar{p}K^- \pi^+$ decay process.

To obtain the $B^- \rightarrow K^- \Lambda_c^+ \bar{\Lambda}_c^-$ signal yields, we perform an unbinned 2D simultaneous extended maximum-likelihood fit to the ΔM_B versus M_{bc} distributions for the five reconstructed Λ_c decay modes. The mass difference ΔM_B is defined as $M_B - m_B$, where M_B is the invariant mass of the B candidate and m_B is the nominal B -meson mass. The beam-energy-constrained mass M_{bc} is defined as $\sqrt{E_{\text{beam}}^2/c^2 - (\sum \vec{p}_i)^2/c^2}$, where E_{beam} is the beam energy and \vec{p}_i are the three-momenta of the B -meson decay products, all defined in the center-of-mass system. Figure 3 shows the 2D distribution and projections of the fit superimposed on the M_{bc} and ΔM_B distribu-

tions, summing over all five reconstructed Λ_c decay modes. We observe 153 ± 14 signal events with a signal significance above 10σ , and extract the branching fraction of $\mathcal{B}(B^- \rightarrow K^- \Lambda_c^+ \bar{\Lambda}_c^-) = [4.80 \pm 0.43(\text{stat}) \pm 0.60(\text{syst})] \times 10^{-4}$. This result has a much-improved precision comparing to the previous measurements done by BaBar [10] and Belle [14].

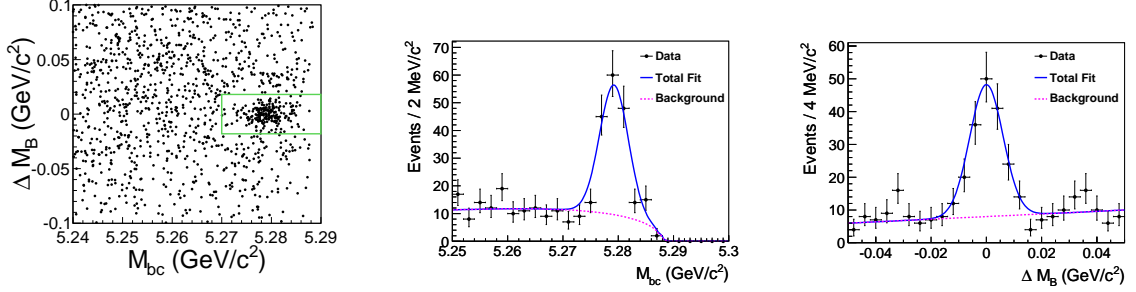


Figure 3: Signal-enhanced distribution of ΔM_B versus M_{bc} (left) and its projections (center and right) from the selected $B^- \rightarrow K^- \Lambda_c^+ \bar{\Lambda}_c^-$ candidates, summing over all five reconstructed Λ_c decay modes. The signal region is indicated by green box.

An unbinned simultaneous extended maximum-likelihood fit is performed to the $K^- \Lambda_c^+$ invariant mass spectra for selected B^- and Λ_c^- -signal events and the Λ_c^+ and $\bar{\Lambda}_c^-$ mass sidebands. The fit results are shown in Fig. 4 (left). The fitted mass and width of the $\Xi_c(2930)$ are $M_{\Xi_c(2930)} = 2928.9 \pm 3.0(\text{stat})_{-12.0}^{+0.9}(\text{syst})$ MeV/c² and $\Gamma_{\Xi_c(2930)} = 19.5 \pm 8.4(\text{stat})_{-7.9}^{+5.9}(\text{syst})$ MeV. The significance of the fit is 5.2σ .

The $M_{\Lambda_c^+ \bar{\Lambda}_c^-}$ spectrum is shown in Fig. 4 (center and right), in which no clear Y_η or $Y(4660)$ signals is evident. An unbinned extended maximum-likelihood fit is applied to the $\Lambda_c^+ \bar{\Lambda}_c^-$ mass spectrum to extract the signal yields of the Y_η and $Y(4660)$ in B decays. In the fit, the signal shape of the Y_η or $Y(4660)$ is obtained from MC simulation directly with the input parameters $M_{Y_\eta} = 4616$ MeV/c² and $\Gamma_{Y_\eta} = 30$ MeV, and $M_{Y(4660)} = 4643$ MeV/c² and $\Gamma_{Y(4660)} = 72$ MeV. From the fits, we have 10 ± 23 Y_η signal events with a statistical signal significance of 0.7σ , and -10 ± 26 $Y(4660)$ signal events. As the statistical signal significance of each Y state is less than 3σ , 90% C.L. Bayesian upper limits on $\mathcal{B}(B^- \rightarrow K^- Y) \mathcal{B}(Y \rightarrow \Lambda_c^+ \bar{\Lambda}_c^-)$ are determined to be 1.2×10^{-4} and 2.0×10^{-4} for $Y = Y_\eta$ and $Y(4660)$, respectively.

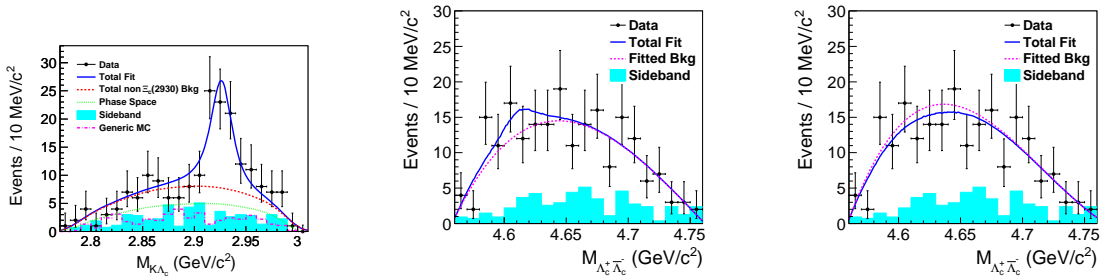


Figure 4: The $M_{K^- \Lambda_c^+}$ distribution of the selected data candidates, with fit results superimposed (left). The $\Lambda_c^+ \bar{\Lambda}_c^-$ invariant mass spectra in data with Y_η (center) and $Y(4660)$ (right) signals included in the fits.

3. Measurement of branching fractions of hadronic decays of the Ω_c^0 baryon

The Ω_c^0 comprises the combination of a charm quark and two strange quarks. The two spectator quarks of the Ω_c^0 have the same flavor, and this leads to many decay diagrams producing the same final states. Constructive interference among these diagrams is thought to explain the short lifetime, despite the fact that, unlike other charmed baryons, it cannot decay via a Cabibbo-favored W-exchange diagram. Measuring the branching fractions of all the charmed hadrons helps to disentangle the various processes involved and adds to our knowledge of the dynamics of charmed baryon decays.

We present the most precise measurements of the branching fractions of Ω_c^0 decays into four decay modes ($\Omega^- \pi^+ \pi^0$, $\Omega^- \pi^+ \pi^- \pi^+$, $\Xi^- K^- \pi^+ \pi^+$, $\Xi^- \bar{K}^0 \pi^+$). These modes have previously been measured by the CLEO [15] and/or BaBar [16] Collaborations. We also present the measurement of three previously unreported decays ($\Xi^- \bar{K}^0 \pi^+$, $\Xi^0 \bar{K}^0$ and $\Lambda \bar{K}^0 \bar{K}^0$) and a search for one other decay, $\Sigma^+ K^- K^- \pi^+$, that was reported by the E687 Collaboration [17]. All branching fractions are measured relative to the decay $\Omega_c^0 \rightarrow \Omega^- \pi^+$.

Figure 5 shows the invariant mass distributions for eight Ω_c^0 decay modes. Many of the modes under consideration may have resonant substructure that can help to reveal their decay mechanisms. Figure 6(a) shows the $\pi^+ \pi^0$ invariant mass in the $\Omega_c^0 \rightarrow \Omega^- \pi^+ \pi^0$ mass distribution. A fit is made to this distribution using the sum of a ρ^+ signal shape and a nonresonant shape flat in phase space. For the mode $\Omega_c^0 \rightarrow \Xi^- K^- \pi^+ \pi^+$, we present the scaled sideband-subtracted $\Xi^- \pi^+$ and $K^- \pi^+$ invariant mass distributions in Figs. 6(b) and 6(c). Polynomial nonresonant functions are fit to these distributions to find the yield of $\Xi^0(1530)$ and $\bar{K}^{*0}(892)$, respectively. For the mode $\Omega_c^0 \rightarrow \Xi^0 K^- \pi^+$, we plot the sideband-subtracted $K^- \pi^+$ invariant mass distribution and observe a clear peak due to the $\bar{K}^{*0}(892)$ meson. The sum of a $\bar{K}^{*0}(892)$ signal shape and a polynomial nonresonant shape is fit to this distribution and shown in Fig. 6(d).

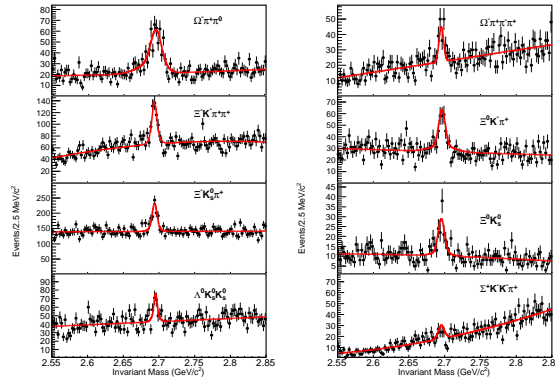


Figure 5: Invariant mass distributions for the eight Ω_c^0 decay modes under consideration.

Results for the branching fractions are summarized in Table 2. These new measurements are consistent, within two standard deviations, with the previous measurements [9] and provide substantial improvements in precision.

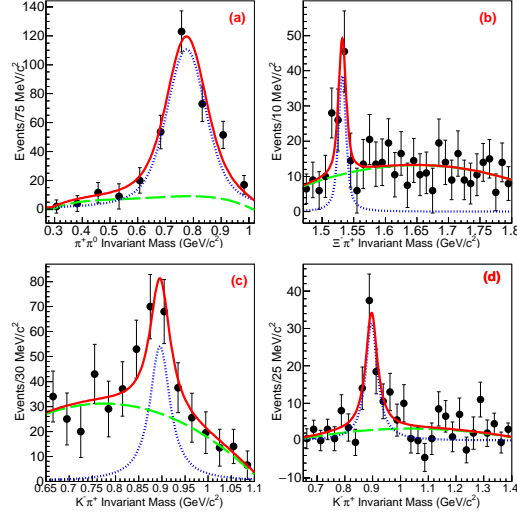


Figure 6: Background-subtracted invariant mass distributions for two-particle combinations: (a) $\pi^+\pi^0$ for $\Omega_c^0 \rightarrow \Omega^-\pi^+\pi^0$ decays, (b) $\Xi^-\pi^+$ and (c) $K^-\pi^+$ for $\Omega_c^0 \rightarrow \Xi^-K^-\pi^+\pi^+$ decays, and (d) $K^-\pi^+$ for $\Omega_c^0 \rightarrow \Xi^0K^-\pi^+$ decays. The blue dotted lines show the signals, the green dashed lines show the background, and the solid lines the sum of the two. Data are shown with circles.

Mode	Branching ratio with respect to $\Omega^-\pi^+$	Substructure	Previous measurement
$\Omega^-\pi^+$	1		
$\Omega^-\pi^+\pi^0$	$2.00 \pm 0.17 \pm 0.11$		$1.27 \pm 0.3 \pm 0.11$
$\Omega^-\rho^+$		$> 71\%$	
$\Omega^-\pi^+\pi^-\pi^+$	$0.32 \pm 0.05 \pm 0.02$		$0.28 \pm 0.09 \pm 0.01$
$\Xi^-K^-\pi^+\pi^+$	$0.68 \pm 0.07 \pm 0.03$		$0.46 \pm 0.13 \pm 0.03$
$\Xi^0(1530)K^-\pi^+$		$(33 \pm 9)\%$	
$\Xi^-\bar{K}^{*0}\pi^+$		$(55 \pm 16)\%$	
$\Xi^0K^-\pi^+$	$1.20 \pm 0.16 \pm 0.08$		$4.0 \pm 2.5 \pm 0.4$
$\Xi^0\bar{K}^{*0}$		$(57 \pm 10)\%$	
$\Xi^-\bar{K}^0\pi^+$	$2.12 \pm 0.24 \pm 0.14$		
$\Xi^0\bar{K}^0$	$1.64 \pm 0.26 \pm 0.12$		
$\Lambda\bar{K}^0\bar{K}^0$	$1.72 \pm 0.32 \pm 0.14$		
$\Sigma^+K^-K^-\pi^+$	< 0.32 (90% CL)		

Table 2: The summary of the results. The numbers in parentheses refer to the fraction of the multibody final state that includes the listed resonance. Previous measurements are performed by BaBar [16] and CLEO [15].

4. Observation of excited Ω_c charmed baryons in e^+e^- collisions

Recently, the LHCb collaboration announced the discovery of five narrow resonances in the final state $\Xi_c^+K^-$ [18]. In addition, they showed a wide enhancement at the higher mass of 3.188 GeV/ c^2 , which may comprise more than one state. Here we present the results of an analysis of the same final state using data from the Belle experiment, and confirm many of the LHCb discoveries.

Seven different Ξ_c^+ decay modes are considered – $\Xi^-\pi^+\pi^+$, $\Lambda K^-\pi^+\pi^+$, $\Xi^0\pi^+$, $\Xi^0\pi^+\pi^-\pi^+$, $\Sigma^+K^-\pi^+$, $\Lambda K_S^0\pi^+$, and $\Sigma^0 K_S^0\pi^+$.

Figure 7(a) shows the invariant mass distribution of the $\Xi_c^+ K^-$ combinations in the mass range of interest, which starts at the kinematic threshold. The masses and intrinsic widths of all six resonances are fixed to the values found by LHCb. We use an unbinned likelihood fit. Figure 7(b) shows the same distribution for wrong-sign, *i.e.* $\Xi_c^+ K^+$ combinations. Figure 7(c) shows the same distribution using Ξ_c^+ candidates with reconstructed masses three to five standard deviations from the canonical mass.

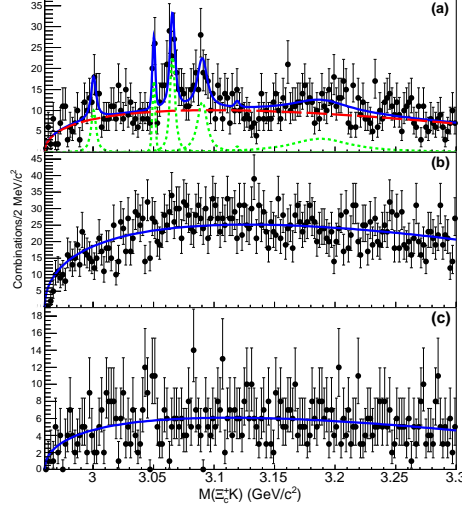


Figure 7: (a) The $\Xi_c^+ K^-$ invariant mass distribution. The fit shown by the solid line is the sum of a threshold function (dashed line) and six Voigtian (Breit-Wigner convolved with Gaussian resolution) functions, with fixed masses, intrinsic widths and resolutions (dotted lines). (b) A threshold function fit to the $\Xi_c^+ K^+$ (wrong-sign) invariant mass distribution. (c) A threshold function fit to the invariant mass distribution for sidebands to the Ξ_c^+ candidates in combination with K^- candidates.

Table 3 shows the yield for each of the five narrow resonances and the wide enhancement reported by LHCb. We can measure the masses of the five confirmed signals, by fitting the same distribution without constraining the masses. In all cases, the masses we find are consistent with the LHCb values, as shown in Table 3.

Ω_c excited state	3000	3050	3066	3090	3119	3188
Yield	37.7 ± 11.0	28.2 ± 7.7	81.7 ± 13.9	86.6 ± 17.4	3.6 ± 6.9	135.2 ± 43.0
Significance	3.9σ	4.6σ	7.2σ	5.7σ	0.4σ	2.4σ
LHCb mass	$3000.4 \pm 0.2 \pm 0.1$	$3050.2 \pm 0.1 \pm 0.1$	$3065.5 \pm 0.1 \pm 0.3$	$3090.2 \pm 0.3 \pm 0.5$	$3119 \pm 0.3 \pm 0.9$	$3188 \pm 5 \pm 13$
Belle mass (with fixed Γ)	$3000.7 \pm 1.0 \pm 0.2$	$3050.2 \pm 0.4 \pm 0.2$	$3064.9 \pm 0.6 \pm 0.2$	$3089.3 \pm 1.2 \pm 0.2$	-	$3199 \pm 9 \pm 4$

Table 3: Yields of the six resonances, and comparison of the mass measurements to the LHCb values. In rows 4 and 5, the units are MeV/c^2 . None of the mass measurements include the uncertainty in the ground-state Ξ_c^+ which is common to both experiments.

It is clear that these data unambiguously confirm the existence of the $\Omega_c(3066)$ and $\Omega_c(3090)$. Signals of reasonable significance are seen for the $\Omega_c(3000)$ and the $\Omega_c(3050)$, but no signal is apparent for the $\Omega_c(3119)$. There is an excess in the Belle data around $3.188 \text{ GeV}/c^2$, which may (as was the case in the LHCb data) be due to one or more particles.

References

- [1] M. Berger *et al.* (Belle Collaboration), *Measurement of the decays $\Lambda_c \rightarrow \Sigma\pi\pi$ at Belle*, submitted to PRD [hep-ex/1802.03421].
- [2] Y.B. Li *et al.* (Belle Collaboration), *Observation of $\Xi_c(2930)^0$ and updated measurement of $B^- \rightarrow K^- \Lambda_c^+ \bar{\Lambda}_c^-$ at Belle*, Eur. Phys. J. C **78** (2018) no.3, 252 [hep-ex/1712.03612].
- [3] J. Yelton *et al.* (Belle Collaboration), *Measurement of branching fractions of hadronic decays of the Ω_c^0 baryon*, Phys. Rev. D **97**, 032001 (2018) [hep-ex/1712.01333].
- [4] J. Yelton *et al.* (Belle Collaboration), *Observation of Excited Ω_c Charmed Baryons in e^+e^- Collisions*, Phys. Rev. D **97**, 051102 (2018) [hep-ex/1711.07927].
- [5] A. Abashian *et al.* (Belle Collaboration), *The Belle Detector*, Nucl. Instr. and Meth. A **479**, 117 (2002); also see detector section in J. Brodzicka *et al.*, *Physics Achievements from the Belle Experiment*, Prog. Theor. Exp. Phys. **2012**, 04D001 (2012) [hep-ex/1212.5342].
- [6] S. Kurokawa and E. Kikutani, *Overview of the KEKB accelerators*, Nucl. Instr. and Meth. A **499**, 1 (2003), and other papers included in this volume; T. Abe *et al.*, *Achievements of KEKB*, Prog. Theor. Exp. Phys. **2013**, 03A001 (2013) and references therein.
- [7] A. Zupanc *et al.* (Belle Collaboration), *Measurement of the Branching Fraction $\mathcal{B}(\Lambda_c^+ \rightarrow pK^- \pi^+)$* , Phys. Rev. Lett. **113**, 042002 (2014) [hep-ex/1312.7826].
- [8] M. Ablikim *et al.* (BESIII Collaboration), *Measurements of absolute hadronic branching fractions of Λ_c^+ baryon*, Phys. Rev. Lett. **116** (5), 052001 (2016) [hep-ex/1511.08380].
- [9] M. Tanabashi *et al.* (Particle Data Group), *The Review of Particle Physics*, Phys. Rev. D **98**, 030001 (2018).
- [10] B. Aubert *et al.* (BaBar Collaboration), *A Study of $\bar{B} \rightarrow \Xi_c \bar{\Lambda}_c^-$ and $\bar{B} \rightarrow \Lambda_c^+ \bar{\Lambda}_c^- \bar{K}$ decays at BABAR*, Phys. Rev. D **77**, 031101 (2008) [hep-ex/0710.5775].
- [11] G. Pakhlova *et al.* (Belle Collaboration), *Observation of a near-threshold enhancement in the $e^+e^- \rightarrow \Lambda_c^+ \Lambda_c^-$ cross section using initial-state radiation*, Phys. Rev. Lett. **101**, 172001 (2008) [hep-ex/0807.4458].
- [12] X. L. Wang *et al.* (Belle Collaboration), *Observation of Two Resonant Structures in $e^+e^- \rightarrow \pi^+ \pi^- \psi(2S)$ via Initial State Radiation at Belle*, Phys. Rev. Lett. **99**, 142002 (2007) [hep-ex/0707.3699].
- [13] F. K. Guo, J. Haidenbauer, C. Hanhart, and U. G. Meiner, *Reconciling the $X(4630)$ with the $Y(4660)$* , Phys. Rev. D **82**, 094008 (2010) [hep-ph/1005.2055].
- [14] K. Abe *et al.* (Belle Collaboration), *Observation of $B^+ \rightarrow \Lambda_c^+ \Lambda_c^- K^+$ and $B^0 \rightarrow \Lambda_c^+ \Lambda_c^- K^0$ decays*, Phys. Rev. Lett. **97**, 202003 (2006) [hep-ex/0508015].
- [15] D. Cronin-Hennessy *et al.* (CLEO Collaboration), *Observation of the Ω_c^0 charmed baryon at CLEO*, Phys. Rev. Lett. **86**, 3730 (2001) [hep-ex/0010035].
- [16] B. Aubert *et al.* (BaBar Collaboration), *Production and decay of Ω_c^0* , Phys. Rev. Lett. **99**, 062001 (2007) [hep-ex/0703030].
- [17] P. Frabetti *et al.*, (E687 Collaboration), *Observation and mass measurement of $\Omega_c^0 \rightarrow \Sigma^+ K^- K^- \pi^+$* , Phys. Lett. B **338**, 106 (1994).
- [18] R. Aaij *et al.* (LHCb Collaboration), *Observation of five new narrow Ω_c^0 states decaying to $\Xi_c^+ K^-$* , Phys. Rev. Lett. **118**, 182001 (2017) [hep-ex/1703.04639].